AGU PUBLICATIONS

Geophysical Research Letters

RESEARCH LETTER
10.1002/2016GL070754

Key Points:
- A meteotsunami index linking meteotsunami wave height to synoptic atmospheric conditions is constructed
- The probability of meteotsunami occurrence can be forecasted from synoptic atmospheric patterns
- The probability rate of meteotsunami occurrence can be estimated for past and future climates

Correspondence to:
J. Šepić,
sepic@izor.hr

Citation:
Šepić, J., I. Vilibić, and S. Monserrat (2016), Quantifying the probability of meteotsunami occurrence from synoptic atmospheric patterns, *Geophys. Res. Lett.*, *43*, doi:10.1002/2016GL070754.

Received 5 AUG 2016
Accepted 22 SEP 2016
Accepted article online 23 SEP 2016

Quantifying the probability of meteotsunami occurrence from synoptic atmospheric patterns

Jadranka Šepić[1], Ivica Vilibić[1], and Sebastian Monserrat[2]

[1]Institute of Oceanography and Fisheries, Split, Croatia, [2]Department of Physics, University of the Balearic Islands, Palma, Spain

Abstract A synoptic atmospheric index is constructed for the region of the Balearic Islands, Spain. The index links the occurrence of meteotsunamis, i.e., atmospherically induced high-frequency sea level oscillations (2 min $< T <$ 120 min), to contemporaneous meteorological synoptic conditions above the region. The correlation between the synoptic index and wave heights is found to be significant and high (up to 0.75). The vertical wind profile is recognized as the most important variable governing the sea level response to atmospheric conditions. The probability of the occurrence of a meteotsunami can be then evaluated from synoptic atmospheric variables. The results show that there exists an index threshold, below which the probability for an intense meteotsunami occurrence is extremely low. However, meteotsunami-favorable synoptic conditions (the index exceeding the threshold value) are crucial but insufficient; some mesoscale features, not reflected in the synoptic pattern, are found to play an important role in meteotsunami generation. The constructed index is potentially applicable to other world locations where a set of tsunamigenic synoptic conditions may be defined in a similar way as at the Balearic Islands. The index can be used to estimate the rate of meteotsunami occurrence under the conditions of past, present, and future climates. It can also be effectively used in meteotsunami warning systems, especially to switch between a "silent mode" (index below the threshold value) to an "event mode."

1. Introduction

Owing to the vast network of seismographs, tide gauges and deep-ocean-bottom pressure sensors incorporated into modern warning systems and real-time decision-making processes, most of today's tsunamis come with an advance warning [*Kânoğlu et al*., 2015]. In contrast, meteorological tsunamis (or meteotsunamis), i.e., tsunami-like waves of atmospheric origin [*Monserrat et al*., 2006], usually come without a timely alert, causing unexpected damage. Every now and then, meteotsunamis can cause severe destruction and loss of lives [*Ewing et al*., 1954; *Hibiya and Kajiura*, 1982]. Due to their unexpectedness, meteorological tsunamis often give rise to panic and speculation [*Okal et al*., 2014; *Šepić et al*., 2015].

Meteorological tsunamis have been observed at the coasts of all continents, except for Antarctica [*Pattiaratchi and Wijeratne*, 2015; *Vilibić et al*., 2016]. As recently as 2014, several locations around the world were hit by sudden and damaging meteotsunamis: Praia do Cassino Beach in Brazil (9 February) [*Vilibić et al*., 2016]; Panama City, Florida, USA (28 March) [http://www.extremestorms.com/meteo_tsunami.htm]; and Fremantle Harbor in Australia (17 August) [*Pattiaratchi and Wijeratne*, 2015]. The latter event caused a cargo ship to crash into a major rail bridge, closing it for 2 weeks. The most dramatic of the 2014 events occurred in the Mediterranean and Black Seas during the last week of June, when a number of harbors and beaches were struck by a series of strong meteotsunami waves [*Šepić et al*., 2015].

Meteorological tsunamis are produced by atmospheric pressure disturbances through resonant processes that facilitate the generation and growth of long-ocean waves at tsunami frequencies. These disturbances are characterized by a sudden change of air pressure (~2–5 hPa/10 min) and are related to (i) small-scale atmospheric processes, e.g., convective clouds, squall lines, isolated atmospheric pressure jumps, or trains of atmospheric gravity waves [*Rabinovich and Monserrat*, 1996, 1998; *Jansà et al*., 2007; *Belušić et al*., 2007; *Tanaka*, 2010], or (ii) processes occurring over a much larger scale, such as tropical storms [*Mercer et al*., 2002], deep cyclones [*Bechle et al*., 2015], and derechos [*Šepić and Rabinovich*, 2014].

During meteorological tsunamis, atmospheric conditions are predominantly characterized by some specific synoptic features. The most relevant one is the presence of strong middle-upper air winds (approximately at pressure levels of 300 to 500 hPa). This has been noticed for meteotsunamis occurring on the western

[*Thomson et al*., 2009] and eastern [*Šepić and Rabinovich*, 2014] coasts of North America, and in South America [*Dragani et al*., 2002], Portugal [*Santos et al*., 2014], the Mediterranean [*Jansà et al*., 2007; *Vilibić and Šepić*, 2009], and Japan [*Tanaka*, 2010].

Strong upper air winds are known as a possible source of instabilities and can lead to the generation of pronounced atmospheric disturbances [*Uccellini and Koch*, 1987; *Plougonven and Zhang*, 2014]. These disturbances are furthermore commonly guided by the upper layer winds, thus propagating with the same wind velocity. The velocity of propagation of an atmospheric disturbance is a key factor in determining the response of the sea level to this atmospheric forcing. Those disturbances, propagating with the speed c of long ocean waves ($c = \sqrt{gh}$, where g is the acceleration due to gravity and h is the sea depth), can resonantly enhance long-ocean waves and thus generate a strong sea level response [*Proudman*, 1929].

Additional tsunamigenic synoptic features have been recognized at several locations worldwide. Most of the synoptic studies have so far been performed for the Mediterranean, where meteorological tsunamis occur under particular conditions [*Jansà et al*., 2007; *Šepić et al*., 2015]. These conditions include (1) the inflow of warm and dry air in the lower troposphere commonly associated with a (2) near-surface temperature inversion and (3) weak surface cyclone and winds, and (4) strong midtropospheric winds embedded in (5) unstable atmospheric layers. These conditions favor the generation [*Šepić et al*., 2015] and propagation of meteotsunamigenic pressure disturbances through wave ducting in the lower troposphere [*Monserrat and Thorpe*, 1996].

The identification of tsunamigenic synoptic settings has so far been purely qualitative. This study aims to quantify the relationship between favorable synoptic features and observation of meteorological tsunamis by constructing a synoptic meteotsunami index. This index is a function of selected synoptic variables that best describe the atmospherically induced sea level oscillations at the tsunami frequency range for a given location. If reliable relationships are determined for a given region, then a timely probabilistic meteotsunami warning may be provided. This also enables the estimation of the rate of occurrence of these oscillations in past and future climates, thus facilitating estimates of sea level extremes.

In this paper, we construct a synoptic meteotsunami index for the region of Ciutadella (Balearic Islands, Spain), a known meteotsunami "hot spot" [*Monserrat et al*., 2006]. However, the analysis can be repeated in a straightforward manner for any other location for which there are sea level measurements for a sufficient length of time (at least a couple of years) and of sufficiently small sampling interval (at least one per minute). The number of the sea locations has continued to grow in recent years as global 1 min sea level observations have become available through several online portals, such as the Intergovernmental Oceanographic Commission Sea Level Station Monitoring Facility (http://www.ioc-sealevelmonitoring.org) or National Oceanic and Atmospheric Administration Tides and Currents (https://tidesandcurrents.noaa.gov/).

2. Constructing the Meteotsunami Index

ERA-Interim atmospheric fields extracted from 1 January 2013 to 1 January 2016 at 00:00, 06:00, 12:00, and 18:00 UTC are used to construct the meteotsunami index for the region of Ciutadella. The fields considered are as follows: (1) vertical profiles of wind, temperature, and relative humidity from the surface up to a pressure level of 400 hPa at the ERA-Interim grid point closest to Ciutadella (referred to hereafter as Ciutadella point) and (2) horizontal fields of mean sea level pressure (mslp), temperature at 850 hPa, and both wind and geopotential at 550 hPa, all in a rectangular area centered over Ciutadella point, spanning longitudes from −15.00°E to 30.00°E and latitudes from 24.75°N to 55.50°N (Figure 1).

The time evolution of these variables is compared with the sea level time series measured during the same period at Ciutadella by a Geonica MTD-3008P radar tide gauge (Figure 1). Sea level data obtained with a sampling interval of 1 min are first quality checked and then used to construct a wave height time series. Wave heights are estimated as a part of a sea level curve between two successive falling points of inflection. Two series were considered: the wave heights averaged over 6 h intervals centered over 00:00, 06:00, 12:00, and 18:00 UTC to be simultaneous with atmospheric reanalysis fields, which are available at those exact hours, and maximum wave heights measured at the same specific intervals. In the forthcoming analysis, only the results using the 6 h averaged wave heights are presented, as (1) these two parameters are highly correlated with a correlation coefficient of 0.98 ($p < 0.00001$; number of samples = 4075) and (2) slightly better

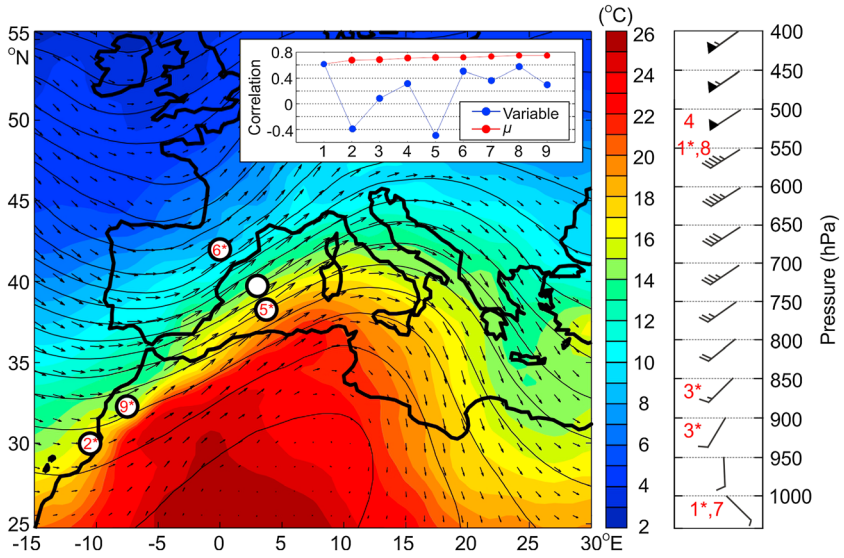

Figure 1. Geographic map showing selected synoptic variables (temperature at 850 hPa and geopotential and wind at 550 hPa) averaged for the 15 strongest events of high-frequency sea level oscillations observed at the Ciutadella tide gauge between 1 January 2013 and 1 January 2016. Averaged vertical wind profile during the same 15 strongest event is shown on the right. The white circle in geographic plot marks the Ciutadella point, and the numbered circles in geographic plot and the numbered heights in vertical wind profile plot stand for positions and heights from which following variables were estimated: (1) vertical difference between wind at 550 hPa and surface wind over Ciutadella point, (2) horizontal mslp difference between Ciutadella point and point 2*, (3) vertical difference between temperature at 850 and 900 hPa over Ciutadella point, (4) relative humidity at 500 hPa over Ciutadella point, (5) horizontal geopotential difference between Ciutadella point and point 5* at 550 hPa, (6) horizontal temperature difference between Ciutadella point and point 6* at 850 hPa, (7) surface wind at Ciutadella point, (8) wind of a 228° direction at 550 hPa in Ciutadella point, (9) horizontal temperature ratio between Ciutadella point and point 9* at 850 hPa. The small inset shows the correlation coefficients between individual variables and wave heights (blue line), and between μ_{1-9} and wave heights (red line)—μ_n is estimated by using the first n variables.

correlations are achieved between meteotsunami indices and wave heights when using 6 h averaging. This better correlation is probably related to a prolonged ringing (over hours to a day) of meteotsunami oscillations in Ciutadella Harbor [*Rabinovich and Monserrat*, 1996, 1998]. Correlations between the time series of atmospheric variables and wave heights are estimated to find optimal variable combinations for constructing the synoptic meteotsunami index. Analyses are performed on the series preprocessed by a 3 day low-pass Kaiser-Bessel window [*Thomson and Emery*, 2014]. We chose a cutoff period of 3 days because the reliability of operational weather forecasts used for correlations is high. When using nonfiltered data or other low-pass filters, the results are comparable.

For each atmospheric variable used to construct the meteotsunami index, we have considered their values at different pressure levels over Ciutadella point, ranging from 1000 to 400 hPa (with a $\Delta p = 25$–50 hPa). We have also computed the vertical differences above Ciutadella point for the indicated pressure levels and horizontal differences between its value at Ciutadella point and all those points included in a box for the region (25°N–55°N, 15°W–30°E) ($\Delta x = \Delta y = 0.75°$). From these computed vertical and horizontal gradients, we have selected those for which the correlation with wave heights is a maximum.

We have thus determined the following nine most significant variables (Figure 1): (1) vertical difference between winds at 550 hPa and 1000 hPa over Ciutadella point, (2) horizontal mslp difference between Ciutadella point and point 2*, (3) vertical temperature difference between 850 and 900 hPa over Ciutadella point, (4) relative humidity at 500 hPa over Ciutadella point, (5) horizontal geopotential difference between Ciutadella point and point 5* at 550 hPa, (6) horizontal temperature difference between Ciutadella point and point 6* at 850 hPa, (7) surface wind at Ciutadella point, (8) wind in a direction of 228° at 550 hPa in Ciutadella point, and (9) horizontal temperature ratio between Ciutadella point and point 9* at 850 hPa. See Figure 1 for the location of the points. The correlation between the time series of these chosen variables and the time series of wave heights were all significant, with a significance level $p < 0.00001$ (sample size = 4075).

We have combined the nine selected variables to construct a set of synoptic meteotsunami indices (μ_n):

$$\mu_n = \sum_{i=1}^{n} A_i x_i. \quad (1)$$

Here n is the number of variables used for construction of μ_n, x_i stands for the variable, and A_i is for the corresponding coefficient. Values of A_i were estimated by using the least squares approach, i.e., by minimizing the function $\sum_{j=1}^{N} \left(h_j - \mu_{nj}\right)$, where N is the number of time steps, h_j is the wave height, and μ_{nj} is the meteotsunami index at the time step j. Altogether, nine versions of μ were estimated. To estimate the meteotsunami index for $n = 1$ (μ_1), the variable chosen was the one with the highest individual correlation with the time series of wave heights (this happened to be the vertical wind difference between 550 hPa and 1000 hPa over Ciutadella point). Then, to construct $n = 2$ index (μ_2), all variables for which the correlation coefficient with the first variable was higher than a given cross-correlation limit (0.1 for μ_2) were not considered. From the remaining variable list, the variable that had the highest correlation with the time series of wave heights was chosen. To construct the $n = 3$ index (μ_3), the first two variables were the same as in μ_2 and the third variable was chosen from a list that excluded all variables having a correlation coefficient with the first and second variables that was higher than the prescribed cross-correlation limit (0.2 for μ_3). The procedure was repeated up through $n = 9$, with the cross-correlation threshold spanning the range from 0 (for μ_1) to 0.8 (for μ_9) (Figure 1), with a step of 0.1. Following this procedure, the nine selected variables were added to construct the meteotsunami indices in the same order as shown in Figure 1.

A meteotsunami index constructed from five variables (μ_5), coinciding with a cross-correlation threshold of 0.4, was chosen as an optimum index and used in all subsequent analysis, which is hereafter referred to as simply μ. In addition, the meteotsunami index has also been reconstructed for the entire ERA-Interim period between 1 January 1979 and 1 January 2016.

3. Hindcast and Forecast of Meteotsunamis

Selected synoptic variables averaged for the 15 strongest meteotsunami events (with maximum measured wave heights between 70.0 and 150.0 cm) at Ciutadella in the period of 2013–2016 are shown in Figure 1. The predominance of this meteotsunamigenic synoptic pattern in the Balearic Islands region is such that the Spanish State Meteorological Agency (AEMET) issues qualitative meteotsunami warnings whenever such a pattern is forecasted [*Jansá*, 1990]. Three different warnings are issued: yellow, orange, and red, corresponding to small, moderate, and high rissaga (the local name for Balearic meteotsunamis), respectively [*Jansá*, 1990]. We aim to advance such a synoptic warning and quantify its reliability by using the meteotsunami index μ.

The μ index is a linear combination of variables (1), (2), (3), (4), and (5), having the respective linear index coefficients of 0.61, −0.39, 0.08, 0.31, and −0.49. The best combination does not include five variables with the highest individual correlations with the wave height time series. This is because some of those highly correlated variables are well correlated with others already selected, and their inclusion thus does not add significant new information to the index. Our results show that the vertical wind profile is a key variable determining the sea level response, specifically, individual correlation of sea level wave heights with vertical wind shear (between 550 hPa and 1000 hPa), and with winds at 550 hPa in a direction of 228° are 0.61 and 0.58, respectively (Figure 1). Only the first variable is included in μ. Wind in the latter direction guides atmospheric disturbances directly toward Ciutadella harbor entrance and is also one of the monitored features of the qualitative meteotsunami warning system developed for the Balearic Islands. The second considered variable is the mean sea level pressure horizontal gradient. This variable reflects the presence of a weak surface cyclone, which is another synoptic feature commonly detected during the Mediterranean meteotsunamis [*Šepić et al*., 2015]. A low-level vertical temperature gradient variable is related to the presence of temperature inversions near the surface. These inversions mark the advection of stable (warm and dry) air masses from the south, thus pointing to the presence of a stable low-troposphere layer necessary for the propagation of atmospheric disturbances [*Monserrat and Thorpe*, 1996]. Midlevel relative humidity has not previously been identified as a key factor in meteotsunami generation over the Balearic Islands. However, this variable is directly related to dynamical instabilities of the midlevels, which is a feature necessary for ducting and propagation of

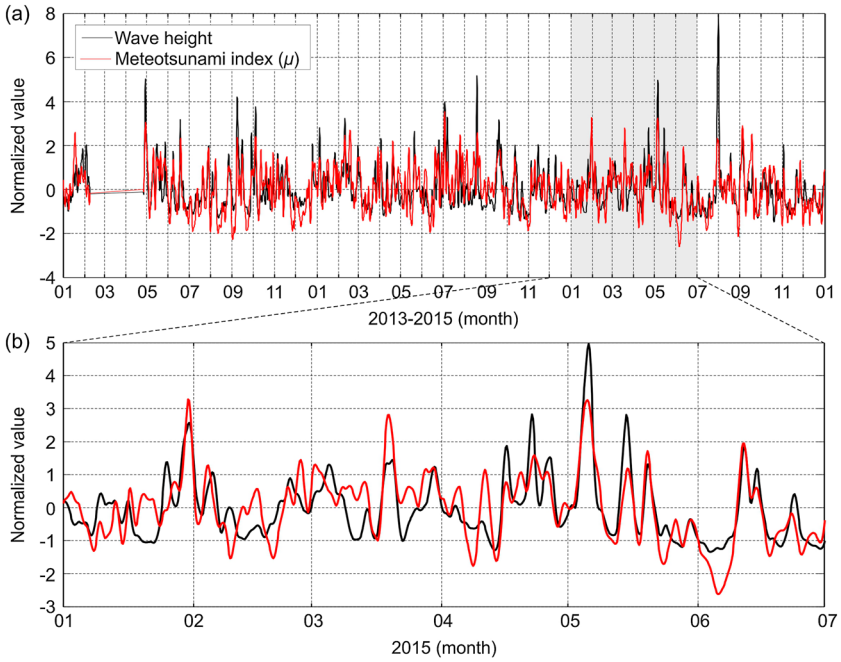

Figure 2. (a) Time series of normalized wave height and normalized meteotsunami index (μ) for 1 January 2013 to 1 January 2016; (b) same as upper but zoomed in for 1 January 2015 to 1 July 2015.

atmospheric pressure disturbances and is commonly detected during Ciutadella meteotsunamis [*Monserrat and Thorpe*, 1996]. The positive correlation with the geopotential horizontal gradient at 550 hPa implies that a strong midtropospheric jet is present directly over the meteotsunami hit area. This is another feature commonly found during the Mediterranean meteotsunamis [*Jansà et al.*, 2007; *Šepić et al.*, 2015]. It is precisely the strong upper layer jet stream that guides the atmospheric pressure disturbances responsible for meteotsunamis [*Monserrat and Thorpe*, 1996].

A time series of normalized μ values and wave heights are shown in Figure 2. The normalization is performed in a standard way by subtracting the mean and dividing the series by the standard deviation. The agreement is satisfactory; the correlation is quite high (0.72) and the onset of oscillations, maximum and minimum times all match. However, the maximum heights of sea level oscillations are not adequately reproduced. In general, the wave heights reach more extreme levels than μ. The relationship between μ and wave height can be even better perceived from a scatter diagram: a linear relation is noticeable (Figure 3). The events with normalized wave heights above 5.0 (6.0), corresponding to maximum measured wave heights of >100.0 (120) cm, happen only when $\mu > 1.6$ (2.0). This implies that a given synoptic background is an *indispensable condition* for the occurrence of a meteotsunami. In contrast, for values of $\mu < 1.6$, no meteotsunamis with maximum measured wave heights above 100.0 cm ($h > 5.0$) were measured. The presence of a synoptic

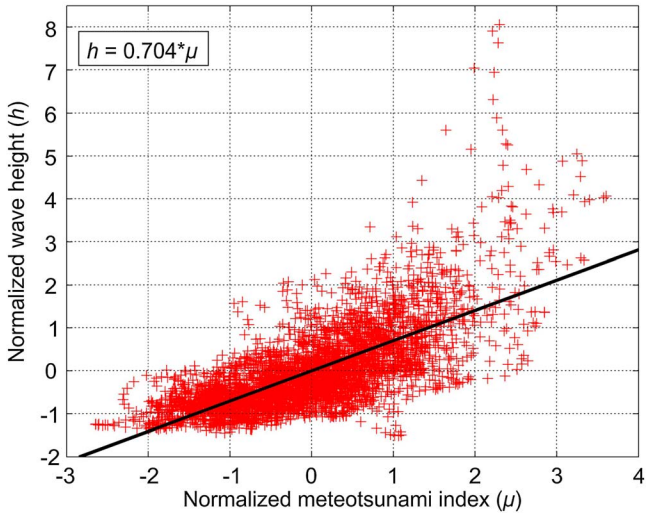

Figure 3. Scatter diagram showing relation between normalized meteotsunami index (μ) and normalized wave height (h) time series. The straight black line (and corresponding equation) shows the linear relation estimated by using linear regression.

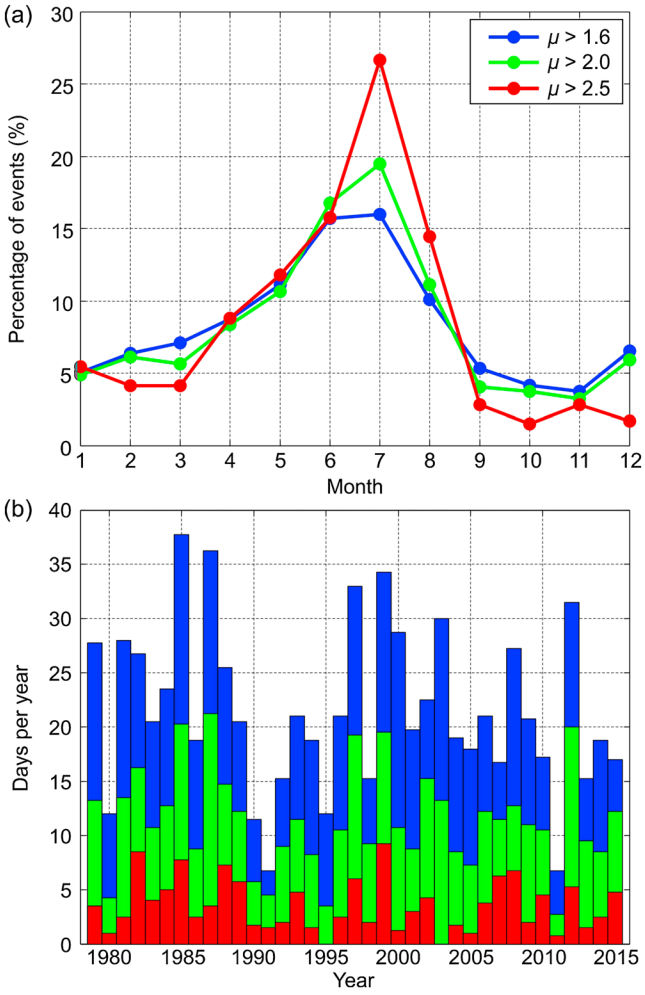

Figure 4. (a) Percentage of synoptic situations with $\mu > 1.6$ (2.0, 2.5) per month. (b) Number of days per year with $\mu > 1.6$ (2.0, 2.5). Both estimates are done for the entire ERA-Interim data set (1 January 1979 to 1 January 2016).

meteotsunamigenic pattern is, however, not a sufficient condition for the occurrence of a meteotsunami. Additionally, very specific atmospheric processes not resolvable by synoptic-scale data (e.g., pronounced air pressure disturbance moving with the correct velocity and mesoscale wave ducting) are also necessary for large meteotsunamis to occur. Nonetheless, the synoptic meteotsunami index provides an initial estimate of the probability of the occurrence of a meteotsunami.

Next, we have estimated a hindcast μ for the entire ERA-Interim period. Following the literature [*Šepić et al.*, 2009, and references therein; *Jansà et al.*, 2007] and the analysis done on the 2013–2016 Ciutadella sea level time series, we have identified 15 meteotsunami events with maximum measured or observed wave height above 100 cm. The hindcast meteotsunami index had values higher than $\mu > 1.6$ during all these events, but one which occurred when the maximum measured wave height was 140 cm and $\mu = 1.4$. We found that all destructive events (maximum wave heights of 200–400 cm) occurred for $\mu > 2.0$. In addition, the occurrence rates of hindcast μ per month and per year for the whole ERA-Interim period (1979–2015) are shown in Figure 4. Synoptic situations characterized by high meteotsunami indices ($\mu > 1.6$) are most common during the warm part of the year (May to August), peaking in July. This is in good agreement with the meteotsunami occurrence rate; meteotsunami events peak in the summer months, with the strongest events occurring almost exclusively during June and July [*Rabinovich and Monserrat*, 1996, 1998]. However, tsunamigenic synoptic situations ($\mu > 1.6$) are expected during an average of 21 days per year (from Figure 4), while moderate to strong meteotsunamis (maximum wave heights > 100 cm) are expected only during an average of about 4 days per year (from Figure 2). This points toward a 20% reliability for a warning during meteotsunami-favorable conditions. Nonetheless, it is clear that not all of synoptic situations characterized by $\mu > 2.0$ result in destructive meteotsunamis.

4. Conclusions

The following conclusions, valid for the specific location of Ciutadella, Balearic Islands, are applicable:

1. There exists a minimum of synoptic conditions that are necessary for a meteotsunami occurrence ($\mu > 1.6$ for maximum wave heights of >100.0 cm). If these conditions are not present, meteotsunamis are highly unlikely to occur, implying that synoptic forecasting of the absence of meteotsunamis is highly reliable.
2. In contrast, tsunamigenic synoptic situations ($\mu > 1.6$) do not always imply moderate to strong meteotsunamis. A 20% reliability for a warning during meteotsunami-favorable conditions has been suggested.

Furthermore, no reliable estimates of meteotsunami strength can be obtained solely by synoptic forecasting. Some additional mesoscale features, not included in the synoptic information, are also necessary for a large meteotsunami to occur.

These features also have a major impact on the final meteotsunami strength. The above conclusions are potentially applicable to other locations throughout the world with similar tsunamigenic synoptic conditions (although the exact numbers should be recalculated). However, the following conclusions are likely to be valid for any meteotsunami prone region:

3. A trustworthy meteotsunami warning system must be based on a combination of synoptic forecast, high-resolution atmospheric and ocean modeling combined with real-time measurements [*Vilibić et al*., 2016]. Such a system may use synoptic forecasting as selection criteria for a warning system to perform in a "silent mode" (no meteotsunami warning) or an "event mode" (possible meteotsunami warning). This should be considered by a number of national agencies that are presently trying to develop meteotsunami warning systems (the National Oceanic and Atmospheric Administration in the USA, University of Western Australia in Australia, Balearic Islands Coastal Observing and Forecasting System in Spain, and Institute of Oceanography and Fisheries in Croatia).
4. Climate simulations can be used to estimate the rate of occurrence of tsunamigenic synoptic patterns in future climates. These estimates should be considered for all climate change adaptation projects, along with the projected rise in sea level, for all locations that are subject to a high risk of meteotsunamis.
5. The analysis presents a novel approach for down-scaling the results of numerical simulations: The probability of a high-frequency (period of ~10 min) and a small-scale (spatial extent of ~10 km) event (meteotsunami) can be estimated by using lower frequency (6 h output) and larger-scale (order of ~50 km) numerical simulations. This may be quite important for local to global sea level studies, which all lack quantitative analyses at tsunami timescales [*Church et al*., 2013]. Our analysis allows for proxy-based estimates of atmospherically driven sea level oscillations at tsunami time scales that may be performed in all oceans and basins where multiyear 1 min sea level measurements are available.

Finally, an analogy with existing tsunami warning procedures for submarine earthquakes should be noticed, particularly concerning items (1)–(3). Namely, although significant tsunamis can only be generated by earthquakes with the momentum magnitude $M_w > 7.5$ (equivalent to (1)), not every earthquake with $M_w > 7.5$ produces a tsunami (equivalent to (2)). Furthermore, tsunami warning systems are operating in a silent mode and an event mode following open-water real-time DART station measurements and real-time numerical modeling, resembling our conclusion (3) [cf. *Titov*, 2009]. These similarities may be used convincingly for structuring the procedures for an efficient meteotsunami warning system.

Acknowledgments
We would like to thank Ports de les Illes Balears, Govern de les Illes Balears, Palma de Mallorca for providing us with tide gauge data, and the European Centre for Medium-Range Weather Forecasts for the atmospheric reanalysis data. Comments and corrections suggested by Alexander Rabinovich and an anonymous reviewer greatly improved the manuscript. The study was supported by MESSI project (UKF Grant 25/15). Tide gauge data should be requested from Ports de les Illes Balears, and atmospheric reanalysis data are accessible through the ECMWF web site (www.ecmwf.int).

References

Bechle, A. J., D. A. R. Kristovich, and H. W. Chin (2015), Meteotsunami occurrences and causes in Lake Michigan, *J. Geophys. Res. Oceans*, *120*, 8422–8438, doi:10.1002/2015JC011317.

Belušić, D., B. Grisogono, and Z. Bencetić Klaić (2007), Atmospheric origin of the devastating coupled air-sea event in the east Adriatic, *J. Geophys. Res.*, *112*, D17111, doi:10.1029/2006JD008204.

Church, J. A., et al. (2013), Sea level change, in *Climate Change 2013: The Physical Science Basis*, edited by T. F. Stocker et al., pp. 1137–1216, Cambridge Univ. Press, Cambridge.

Dragani, W. C., C. A. Mazio, and M. N. Nuñez (2002), Sea level oscillations in coastal water of the Buenos Aires province, Argentina, *Cont. Shelf Res.*, *22*, 779–790.

Ewing, M., F. Press, and W. J. Donn (1954), An explanation of the Lake Michigan wave of 26 June 1954, *Science*, *120*, 684–686.

Hibiya, T., and K. Kajiura (1982), Origin of "abiki" phenomenon (kind of seiche) in Nagasaki Bay, *J. Oceanogr. Soc. Jpn.*, *38*, 172–182.

Jansá, A. (1990), Servei experimental de predicció de rissagues, in *Les Rissagues de Ciutadella i Altres Oscillacions de Nivell de la Mar de Gran Amplitud a la Mediterránea*, pp. 85–91 , Inst. Menorqui d'Estudis, Menorca, Spain.

Jansà, A., S. Monserrat, and D. Gomis (2007), The rissaga of 15 June 2006 in Ciutadella (Menorca), a meteorological tsunami, *Adv. Geosci.*, *12*, 1–4.

Kânoğlu, U., V. Titov, E. Bernard, and C. Synolakis (2015), Tsunamis: Bridging science, engineering and society, *Phil. Trans. R. Soc. A*, *373*, 20140369.

Mercer, D., J. Sheng, R. J. Greatbatch, and J. Bobanović (2002), Barotropic waves generated by storms moving rapidly over shallow water, *J. Geophys. Res.*, *107*(C10), 3152, doi:10.1029/2001JC001140.

Monserrat, S., and A. J. Thorpe (1996), Use of ducting theory in an observed case of gravity waves, *J. Atmos. Sci.*, *53*(12), 1724–1736.

Monserrat, S., A. B. Rabinovich, and I. Vilibić (2006), Meteotsunamis: Atmospherically induced destructive ocean waves in the tsunami frequency band, *Nat. Hazards Earth Syst. Sci.*, *6*, 1035–1051.

Okal, E. A., J. N. J. Visser, and C. H. de Beer (2014), The Dwarskersbos, South Africa, local tsunami of August 27, 1969: Field survey and simulation as a meteorological event, *Nat. Hazards*, *74*, 251–268, doi:10.1007/s11069-014-1205-5.

Pattiaratchi, C. B., and E. M. S. Wijeratne (2015), Are meteotsunamis an underrated hazard?, *Phil. Trans. R. Soc. A*, *373*, 20140377.

Plougonven, R., and F. Zhang (2014), Internal gravity waves from atmospheric jets and fronts, *Rev. Geophys*, *52*, 33–76, doi:10.1002/2012RG000419.

Proudman, J. (1929), The effects on the sea of changes in atmospheric pressure, *Geophys. Suppl. Mon. Notices R. Astron. Soc.*, *2*(4), 197–209.
Rabinovich, A. B., and S. Monserrat (1996), Meteorological tsunamis near the Balearic and Kuril Islands: Descriptive and statistical analysis, *Nat. Hazards*, *13*, 55–90.
Rabinovich, A. B., and S. Monserrat (1998), Generation of meteorological tsunamis (large amplitude seiches) near the Balearic and Kuril Islands, *Nat. Hazards*, *18*, 27–55.
Santos, Â., S. Mendes, and J. Corte-Real (2014), Impacts of the storm Hecules in Portugal, *Finisterra, XLIX*, *98*, 197–220.
Šepić, J., and A. Rabinovich (2014), Meteotsunami in the Great Lakes, Chesapeake Bay and on the Atlantic coast of the United States generated by the propagating 'derecho' of 29–30 June 2012, *Nat. Hazards*, *74*, 75–107, doi:10.1007/s11069-014-1310-5.
Šepić, J., I. Vilibić, and S. Monserrat (2009), Teleconnections between the Adriatic and the Balearic meteotsunamis, *Phys. Chem. Earth*, *34*, 928–937.
Šepić, J., I. Vilibić, A. B. Rabinovich, and S. Monserrat (2015), Widespread tsunami-like waves of 23–27 June in the Mediterranean and Black Seas generated by high-altitude atmospheric forcing, *Sci. Rep.*, *5*, 11682, doi:10.1038/srep11682.
Tanaka, K. (2010), Atmospheric pressure-wave bands around a cold front resulted in a meteotsunami in the East China Sea in February 2009, *Nat. Hazards Earth Syst. Sci.*, *10*, 2599–2610.
Thomson, R. E., and W. J. Emery (2014), *Data Analysis Methods in Physical Oceanography*, 3rd ed., 716 pp., Elsevier Science, Amsterdam.
Thomson, R. E., A. B. Rabinovich, I. V. Fine, D. C. Sinnott, A. McCarthy, N. A. S. Sutherland, and L. K. Neil (2009), Meteorological tsunamis on the coasts of British Columbia and Washington, *Phys. Chem. Earth*, *34*, 971–988.
Titov, V. V. (2009), Tsunami forecasting, in *The Sea, Volume 15: Tsunamis*, edited by E. N. Bernard and A. R. Robinson, pp. 371–400, Harvard Univ. Press, Cambridge.
Uccellini, L. W., and S. E. Koch (1987), The synoptic setting and possible energy sources for mesoscale wave disturbances, *Mon. Weather Rev.*, *115*, 721–729.
Vilibić, I., and J. Šepić (2009), Destructive meteotsunamis along the eastern Adriatic coast: Overview, *Phys. Chem. Earth*, *34*, 904–917.
Vilibić, I., J. Šepić, A. B. Rabinovich, and S. Monserrat (2016), Modern approaches in meteotsunami research and early warning, *Front. Mar. Sci*, *3*, 57, doi:10.3389/fmars.2016.00057.